Three-dimensional advanced numerical approaches to the seismic soil and structural response analyses

Conference Paper · November 2015

CITATIONS
0

READS
37

4 authors:

Angelo Amorosi
Sapienza University of Rome
57 PUBLICATIONS **584** CITATIONS
SEE PROFILE

Daniela Boldini
University of Bologna
77 PUBLICATIONS **364** CITATIONS
SEE PROFILE

Annamaria Di Lernia
Politecnico di Bari
10 PUBLICATIONS **11** CITATIONS
SEE PROFILE

Fabio Rollo
Sapienza University of Rome
1 PUBLICATION **0** CITATIONS
SEE PROFILE

Three-dimensional advanced numerical approaches to the seismic soil and structural response analyses

Angelo Amorosi[1], Daniela Boldini[2],
Annamaria di Lernia[3], Fabio Rollo[1]

Abstract

A 3D non-linear finite element approach is developed to study the free-field seismic ground response and the soil-structure interaction (SSI) phenomena at the Lotung site (Taiwan) during the earthquake event occurred on May 20 1986.

The site was extensively instrumented with down-hole and surface accelerometers, these latter located also on a 1/4–scale nuclear power plant containment structure. An advanced constitutive model is adopted for simulating the soil behaviour, while a linear visco-elastic behaviour is assumed for the structural model.

The free-field and SSI analyses are carried out applying both the NS and EW horizontal components of the acceleration time history as recorded at the depth of 47 m b.g.l. The predicted ground response results are in fair agreement with the recorded motion at depth and at the surface. The dynamic response of structure is well captured for this specific seismic event, thus confirming the validity of the numerical approach.

1 Sapienza University of Rome, Italy.

2 University of Bologna, Italy.

3 Technical University of Bari, Italy.

1. Introduction

It is largely recognised that, during an earthquake, the dynamic response of a structure is generally affected by the compliance of the soil-foundation system and its motion is typically different from that experienced by the same structure founded on a rigid base. The main consequence of this interaction is the reduction of the fundamental frequency of the structure and the variation of its damping ratio [1,2].

The soil-structure interaction (SSI) effects have traditionally been evaluated by the substructure method, which separately estimates the kinematic and inertial interaction effects, implicitly assuming linearity in both soil and structure behaviour. Nevertheless, the soil nonlinearity should be accounted for to correctly predict the seismic ground response and the SSI effects, especially when strong motion earthquakes occur. Thus, a complete dynamic analysis becomes more appropriate to study this phenomenon: a realistic non-linear analysis should be carried out in the time domain, consisting in analysing the entire soil-structure system in a single model [3].

In the present paper the back-analysis of the seismic ground response and the SSI phenomena affecting a 1/4-scale nuclear power plant containment structure, as recorded at the Lotung Large-Scale Seismic Test (LSST) site during the May 20 1986 earthquake, is carried out by means of a 3D non-linear finite (FE) model, implemented through the FE code PLAXIS 3D [4]. The non-linear soil behaviour is described by the elasto-plastic hysteretic model *Hardening Soil model with Small-Strain Stiffness* (*HSsmall*) available in the material model library of the FE code, while a linear visco-elastic model is assumed for the structural response.

The *HSsmall* soil constitutive model has recently been adopted for dynamic engineering applications [5,6] and its capability in predicting seismic ground response has been investigated under both mono-directional and multi-directional conditions [7,8]. Furthermore, the 3D numerical approach has been used to perform SSI analyses under mono-directional conditions (i.e. applying only the EW horizontal component of input motion) [9].

In the present study, the 3D numerical analyses are carried out considering the seismic motion multi-directionality. Thus, both EW and

NS horizontal components of the acceleration time history, as recorded by the deepest accelerometer of the down-hole accelerometric array, are applied simultaneously at the base of the FE numerical model. Results of the non-linear analyses are compared to the in-situ recorded down-hole and surface motions and to the acceleration time histories monitored on the 1/4-scale containment structure.

2. The Lotung LSST case study

The Large-Scale Seismic Test (LSST) was a research programme (1985-1990), led by the Electric Power Research Institute (EPRI) in co-operation with the Taiwan Power Company (TPC), consisting in studying the seismic ground response and the dynamic response of two small-scale (1/4-scale and 1/12-scale models) nuclear power plant containment structures. The LSST site was located in Lotung, a highly seismic region in the North-East of Taiwan.

The 1/4-scale containment model was a reinforced concrete cylindrical shell structure of external radius of 10.52 m, with a flat roof slab and a flat bottom basement. The structure is embedded at the depth of 4.57 m below the ground surface. Within the containment model, a steel shell structure simulating a steam generator prototype of a nuclear power plant was installed.

The LSST site and the 1/4-scale containment structure were extensively instrumented to record both soil and structural responses during earthquakes that occurred at the test site.

Concerning the ground instrumentation, two down-hole arrays, extended to a depth of 47 m from ground surface, were installed to record soil motion at different depths, while three surface arrays were placed along three arms (Arm 1, 2 and 3) of radius of about 47 m from the edge of the 1/4-scale model, as depicted in Figure 1 [10].

As far as the 1/4-scale model concerns, four accelerometers were placed on the basement of the containment structure and four at the top surface of the model, along EW and NS diametrical directions. In addition, two accelerometers were placed at the top and the bottom of the steam generator prototype. The monitoring scheme of the 1/4-scale structural model is illustrated in Figure 2 [11].

The LSST site is located on the Lanyang River plain, which lies on two layers of recent alluvium and Pleistocene deposits, overlying a Miocene basement layer situated at 400 m of depth [12].

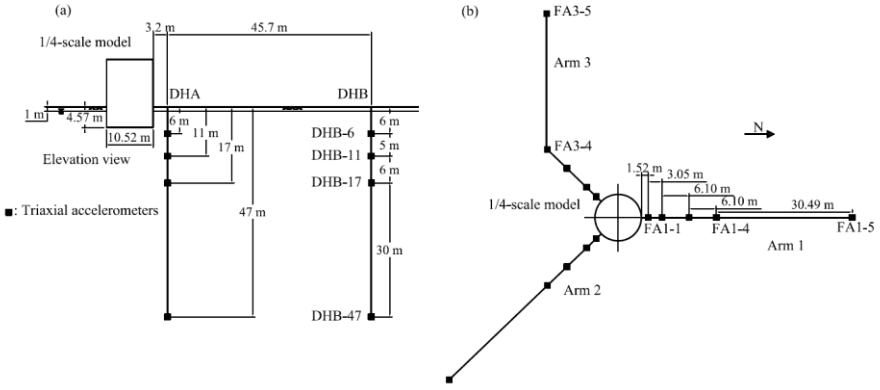

***Figure 1**. Layout of the surface and down-hole instrumentation: (a) down-hole instrument arrays and (b) surface instrument arrays (after Tang*[10]*)*

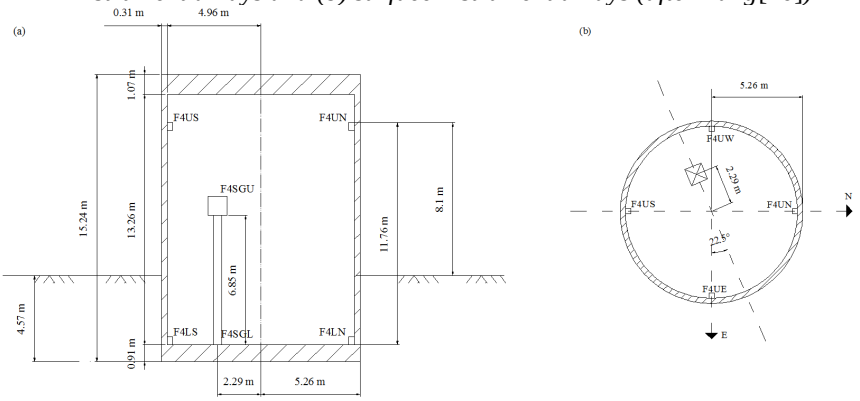

***Figure 2**. Location of accelerometers on the 1/4-scale model of the containment structure: (a) vertical and (b) horizontal cross-section (modified from [11])*

The local geotechnical profile, near the LSST site, is characterized by a layer of silty sand, extended from the ground surface down to about 17 m, above a 6 m thick layer of sand with gravel. Underneath the sandy layer, there is a stratum of silty clay detected by the deepest borehole down to 47 m, interlayered by an inclusion of sand with

gravel between 29 m and 36 m. The water table is intercepted at about 1 m from the ground surface (Figure 3a).

The geotechnical characterisation is based on the few available in situ data and on previously published back-analysed seismic data [11,13–16]. The strength properties of the coarse-grained soils are obtained from SPT tests (Figure 3b), using the correlation proposed by De Mello [17]; due to the lack of direct experimental observations, typical values are assumed for the silty clay layer. A total unit weight of 19.6 kN/m^3 is adopted as an average value for the whole soil deposit [13]. The shear wave velocity profile, obtained from cross-hole tests, ranges from about 100 m/s to 300 m/s at a depth of 47 m, as summarised by Borja et al. [15] (Figure 3c).

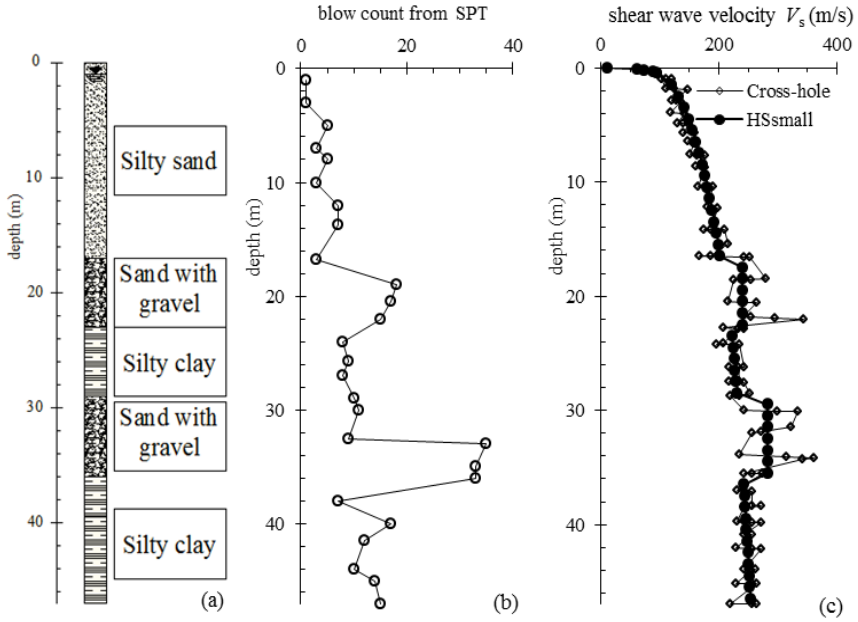

***Figure 3**. Local soil profile at Lotung LSST site: (a) soil stratigraphy; (b) SPT log; (c) shear wave velocity*

The shear modulus and damping ratio curves for the upper silty sand layer are those obtained by Zeghal et al. [14], through an indirect interpretation of 18 earthquakes events occurred between 1985 and 1986. The decay curves obtained at the depth of 11 m (Figure 4a) are assumed in the present FE simulations, as proposed by Borja et al.

[16]. Due to the lack of specific laboratory tests, the shear modulus and damping ratio curves proposed by Vucetic and Dobry [18] for a plasticity index PI equal to 0 and 20 are adopted for the gravelly and the silty-clayey layers, respectively (Figure 4b-c).

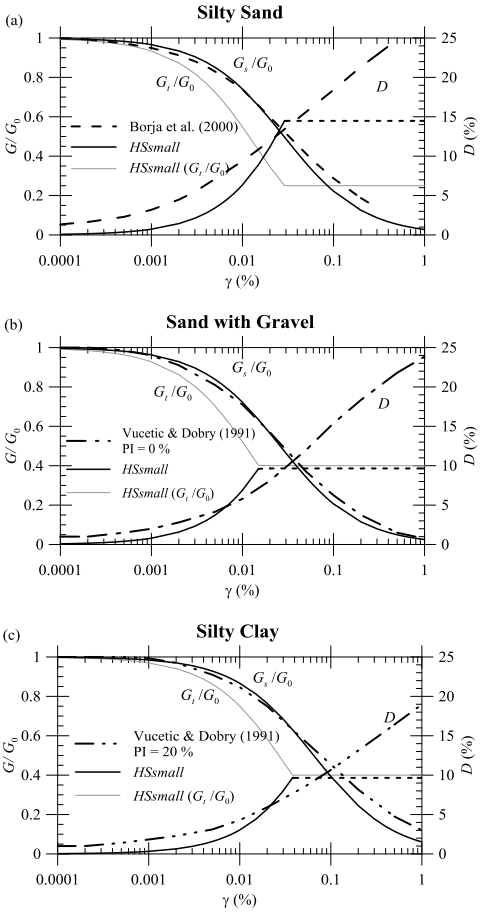

***Figure 4**. Local soil profile at Lotung LSST site: (a) soil stratigraphy; (b) SPT log; (c) shear wave velocity*

In this paper the free-field seismic ground response and the dynamic structural behaviour are investigated with reference to both EW and NS horizontal components of the acceleration time history, as recorded at the depth of 47 m by the accelerometer DHB-47 (Figure 5). The considered earthquake is that occurred on May 20 1986 (LLST7),

whose features are magnitude 6.5, epicentral distance of 66.2 km and duration of 35.48 s.

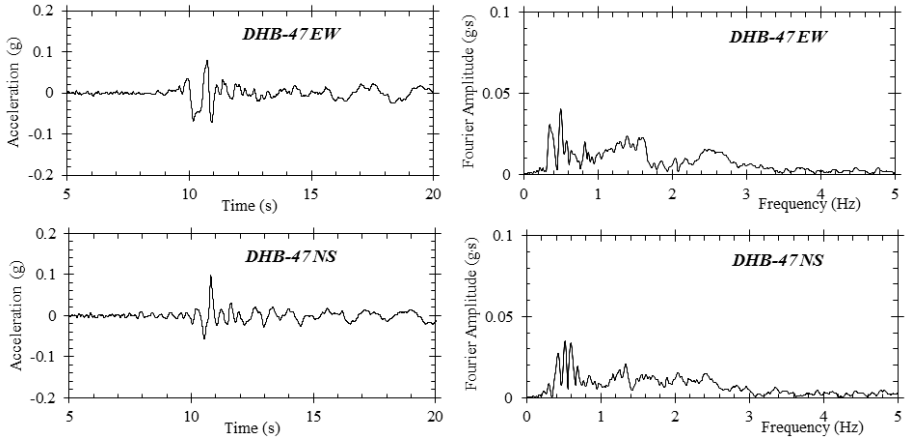

***Figure 5**. EW and NS components of the acceleration time histories and relative Fourier spectra recorded at DHB-47 during LSST7 earthquake*

3. The *HSsmall* soil constitutive model

3.1. Description of the HSsmall model

The soil constitutive model *Hardening Soil model with Small-strain Stiffness* (*HSsmall*) is an evolution of the *Hardening Soil* (*HS*) model, proposed by Schanz et al. [19], extended by the elastic small-strain overlay model, developed by Benz et al. [20,21]. The *HSsmall* model allows to describe the hysteretic para-elastic behaviour of soil at very small strains, by introducing the initial shear stiffness modulus G_0 and the evolution of the secant shear stiffness ratio G_s /G_0 with shear strain γ. The modulus decay curve is implemented as a modified version of the simple hyperbolic law proposed by Hardin and Drnevich [22]

$$\frac{G_s}{G_0} = \frac{1}{1+0.385\dfrac{\gamma}{\gamma_{0.7}}} \tag{1}$$

where $\gamma_{0.7}$ is the deformation at which the secant shear modulus is reduced to about 70% of G_0.

Any variation in the strain increment direction is taken into account by means of a scalar strain history-dependent value, γ_{Hist}, which memorises the deviatoric strain history of the material. Through the strain value γ_{Hist}, a unique value of the tangent stiffness is determined by Eq. (2), which describes the stress-strain relationship along all loading direction in a multi-axial loading condition.

$$\frac{G_t}{G_0} = \frac{G_0}{\left(1 + 0.385 \frac{\gamma}{\gamma_{0.7}}\right)^2} \tag{2}$$

The tangent shear stiffness modulus G_t (Eq. 2) is limited by a lower cut-off value G_{ur}. When the strain level reaches the limit $\gamma_{cut\text{-}off}$ (Eq. 3), the tangent shear stiffness modulus G_t becomes constant and equal to the unloading-reloading shear stiffness modulus $G_{ur} = E_{ur}/2(1+\nu_{ur})$. It results:

$$\gamma_{cut-off} = \frac{\gamma_{0.7}}{0.385}\left(\sqrt{\frac{G_0^{ref}}{G_{ur}^{ref}}} - 1\right) \tag{3}$$

The same lower limit value, G_{ur}, is asymptotically reached by G_s.

Under cyclic conditions, the hysteretic behaviour in unloading-reloading is formulated by the modified Masing's rules, which describe hysteresis loops that gives a measure of energy dissipation [5].

A basic feature of the model is the dependency of the soil stiffness on the stress level, which is implemented as a function of the effective stress and strength parameters c′ and φ':

$$G_0 = G_0^{ref}\left(\frac{c'\cos\varphi' + \sigma_3'\sin\varphi'}{c'\cos\varphi' + p'^{ref}\sin\varphi'}\right)^m \tag{4}$$

where G_0^{ref} is the reference initial shear modulus corresponding to the reference confining pressure p'^{ref} (assumed equal to 100 kPa), m is a constant that depends on soil type and σ_3' is the minor principal effective stress. Similar expressions to Eq. (4) are introduced in the model for the definition of the dependency on the state of stress of the unloading-reloading modulus E_{ur}, the secant stiffness in standard drained triaxial test E_{50} and the tangent stiffness for primary oedometer loading E_{oed}.

The *HSsmall* model is an isotropic hardening elasto-plastic model, characterised by two yield surfaces: a shear hardening yield surface, resembling the hyperbolic law, which can expand up to the Mohr-Coulomb failure criterion as a function of the deviatoric plastic strain; a cap yield surface, introduced to delimit the elastic region for compressive stress paths, which is governed by plastic volumetric strains.

3.2. HS small model parameters calibration

The parameter definition is carried out with reference to the available data, according to a suitable procedure of calibration. The reference initial shear stiffness modulus G_0^{ref} and the parameter *m* are selected to obtain the best fitting with the shear wave velocity profile provided by the cross-hole test (Figure 3c). The shear strain level $\gamma_{0.7}$ is calibrated using the decay curves of shear modulus and damping ratio for the para-elastic response regime (Figure 4). The elastic unloading-reloading shear stiffness modulus G_{ur}^{ref} is determined such that the ratio G_0^{ref} / G_{ur}^{ref} is kept to 4 for the silty sand layer and to 2.5 for the other soil layers, leading to a suitable value of $\gamma_{cut\text{-}off}$. It might be noted that beyond the cut-off shear strain, the damping ratio decreases tending to zero. In fact, beyond this threshold limit, the tangent stiffness modulus becomes constant, but the hysteresis loop becomes narrower for increasing strain levels.

The other stiffness parameters, E_{50}^{ref} and E_{oed}^{ref}, are assumed as three times lower than the elastic unloading-reloading Young's modulus E_{ur}^{ref}, which is evaluated as a function of the Poisson's ratio v_{ur}. For coarse-grained soils, the Poisson's ratio is assumed equal to 0.3, while it is considered equal to 0.25 for the silty soil layers.

The earth pressure coefficient at rest, K_0, is estimated according to the Jâky's expression for coarse-grained soils and according to the expression valid for overconsolidated soil for fine-grained layers. For the sand with gravel and silty sand layers, the overconsolidation ratio OCR is fictitiously set to 10 in order to exclude yielding during radial compressive stress paths.

A summary of the model parameters involved in the numerical analyses is provided in Table 1 for each layer.

***Table 1**. HS small model parameters*

Soil layer	Silty sand (0-17 m)	Sand with gravel (17-23 m)	Silty clay (23-29 m)	Sand with gravel (29-36 m)	Silty clay (36-47 m)
c' (kPa)	0	0	10	0	10
φ' (°)	30	35	24	37	24
OCR	10	10	5	10	5
K_0^{nc}	0.5	0.4264	0.5933	0.3982	0.5933
K_0^{oc}	-	-	1.327	-	1.327
G_0^{ref} (MPa)	90	115	65	160	65
$\gamma_{0.7}$ (%)	0.011	0.01	0.025	0.011	0.025
m	0.54	0	0.42	0	0.42
ν_{ur}	0.3	0.3	0.25	0.3	0.25
E_{ur}^{ref} (MPa)	60	119.5	65	164.5	65
E_{50}^{ref} (MPa)	20	39.83	21.67	54.81	21.67

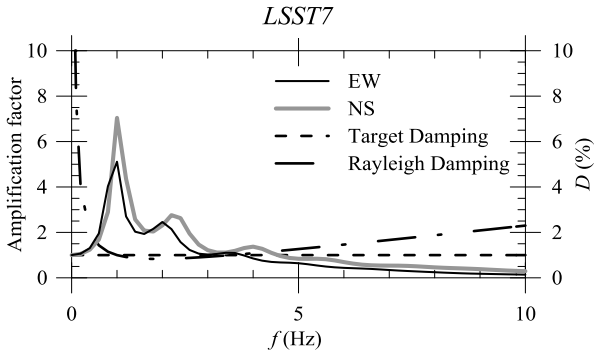

***Figure 6**. Calibration of the Rayleigh viscous damping parameters*

In order to introduce a small amount of damping (of about 1-2%) at very small strain level, viscous damping is added by means of the Rayleigh formulation. The selection of Rayleigh coefficients requires a suitable calibration strategy; here the one proposed by Amorosi et al [23] was adopted, which requires a preliminary equivalent linear analysis, performed by the code EERA [24], in order to determine the amplification functions. Based on the EW amplification function (Figure 6), the first control frequency f_m is identified as the fundamental fre-

quency of the soil deposit (f_m = 1 Hz), while the second control frequency f_n is chosen as the frequency where the amplification function becomes lower than one (f_n = 3.5 Hz).

4. The FE numerical model

The free-field ground response and the dynamic SSI analyses are performed under multi-directional seismic conditions, i.e. applying both EW and NS components of DHB-47 acceleration time history recorded during the LSST7 earthquake.

The geometrical model adopted for the free-field seismic ground response analysis consists of a soil column of width 10 m x 10 m and height equal to 47 m, which is the maximum investigated depth of the soil deposit.

The dynamic SSI analysis is performed using a 47 m thick model, consisting in a soil domain of width equal to 70 m x 70 m. The nuclear power plant containment structure is modelled as a cylindrical plate structure of 0.305 m thickness (the outer diameter is 10.52 m) with two flat circular plate elements at the roof and the bottom, characterised by 1.07 and 0.91 m thickness, respectively.

The structural elements are modelled as linear visco-elastic concrete materials (unit weight of 25 kN/m^3) with Young's modulus $E = 2.53 \cdot 10^4$ MPa and Poisson's ratio $\nu = 0.2$. A structural damping ratio of 2.5 % is assumed and included by means of the simplified Rayleigh formulation ($[C]=\beta_R[K]$). The Rayleigh coefficient β_R is determined selecting a control frequency of 10 Hz, a value close to the fixed-base fundamental frequency of the containment structure.

In both numerical models, the soil domain is divided into 47 layers of unit thickness in the vertical direction, in order to limit the dimension of the elements, according to the requirement that the element size must be smaller than about one/eighth of the wavelength associated with the maximum frequency component f_{max} of the input wave (equal to 10 Hz).

In the pre-seismic static stage, the boundary conditions are characterised by total fixities at the bottom of the mesh, while horizontal displacements are null for the nodes on the vertical sides of the soil domain. In the dynamic phase, *tied nodes* boundary conditions are

adopted, achieved by introducing horizontal node-to-node anchors elements, characterized by high values of axial stiffness *EA* (equal to 10^9 kN). Switching from the static to the dynamic phase triggers a modification of the horizontal constraints, which induces a perturbation of the stress equilibrium. In order to restore it, pressures corresponding to the lithostatic distribution of horizontal effective stresses are introduced on the vertical sides of the mesh. All dynamic analyses are performed under fully undrained conditions.

The Generalized Newmark method is employed, with Newmark parameters β_1 and β_2 equal to 0.6 and 0.605, respectively, ensuring that the algorithm is unconditionally stable.

5. Numerical results

5.1. Free Field ground response

The non-linear numerical results of the free-field wave propagation analyses are compared to the in-situ recorded motion at ground surface (FA1-5) and at the depth of 17 m (DHB-17), in terms of acceleration time histories and relative Fourier spectra for each horizontal component EW and NS (Figure 7).

The predicted response is comparable to the recorded one at the same depths along both horizontal directions, although a general tendency to slightly over-predict the ground motion might be recognised.

A systematic overprediction of the Fourier amplitude around 0.85 Hz can also be observed at all depths, though the frequency content of the signal is satisfactorily reproduced.

The tendency to over-estimate the seismic response should be ascribed to the feature of the constitutive model to provide a reduced amount of hysteretic damping ratio under large multi-directional strain levels, as those induced during the LSST7 earthquake [8]. Related to this behaviour is the generation of significant numerical noise, minimised by adopting a low pass filter (f_{max} = 5 Hz), which was applied to all numerical output signals of the free field numerical analyses.

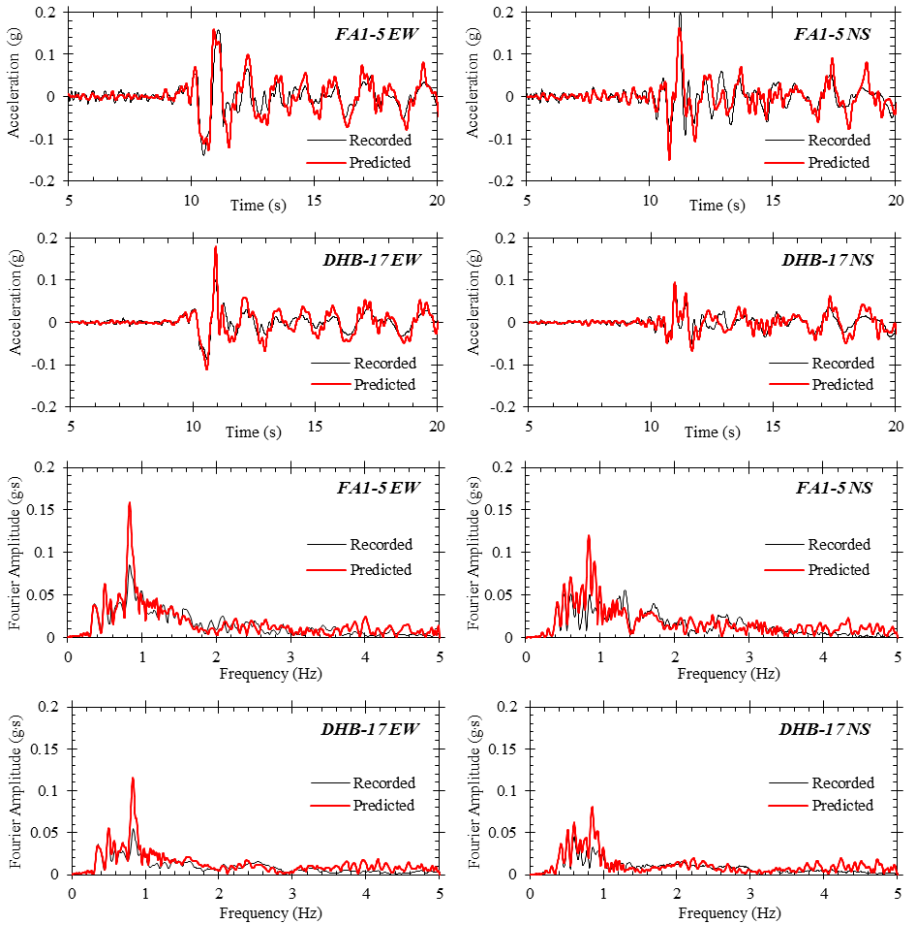

***Figure 7**. Seismic ground motion recorded in-situ and numerically predicted at surface (FA1-5) and at depth of 17 m (DHB-17) along EW and NS horizontal components.*

5.2. Dynamic structural response

The dynamic response of the 1/4-scale model of the containment structure is compared to the that recorded in-situ on the roof (F4U) and at the base (F4L), in terms of acceleration time histories and Fourier amplitude spectra for each horizontal direction (Figure 8).

It appears that the computed response at the bottom of the containment structure matches fairy well that recorded both at F4LW along EW direction and at F4LS along NS direction. Moreover, peak accel-

eration and zero crossings of both acceleration time histories are well predicted by the numerical model. The good prediction is also confirmed by Fourier amplitude spectra.

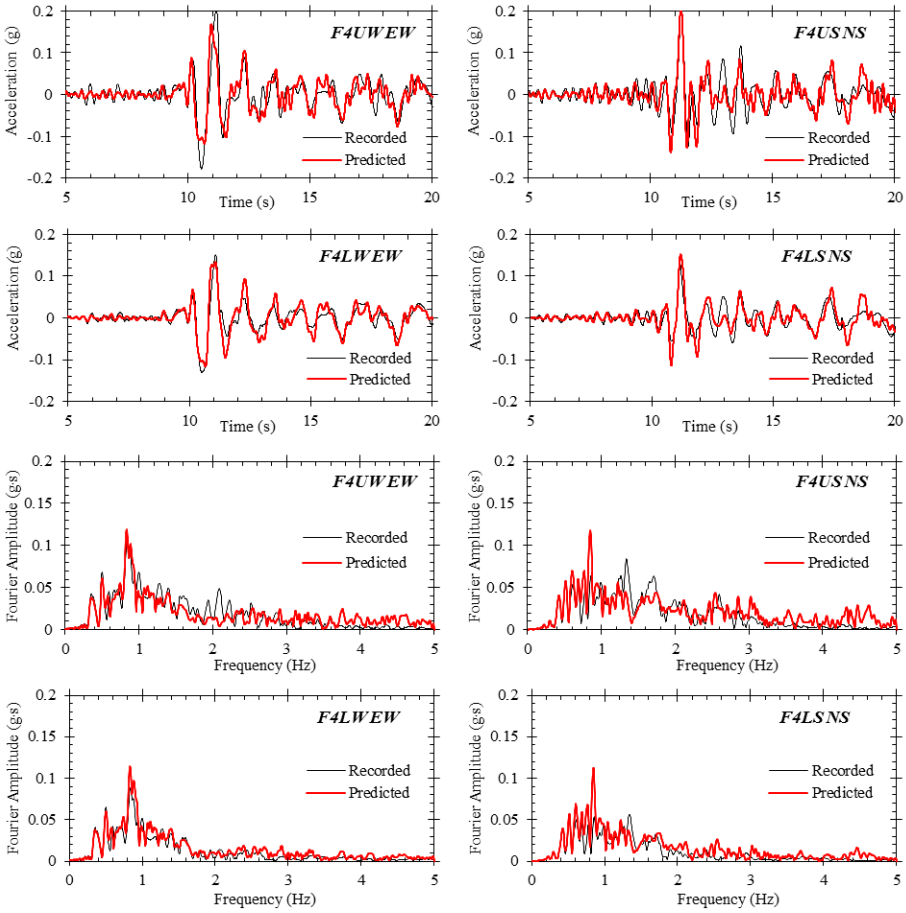

***Figure 8**. Seismic structural motion recorded in-situ and numerically predicted at the roof (F4U) and at the basement (F4L) of the 1/4-scale model of the containment structure along EW and NS horizontal components.*

The predicted dynamic response at the roof of the structure (F4UW EW and F4US NS) is accurately reproduced, especially in the NS horizontal direction, while a slightly underestimation of the peak acceleration might be identified in the EW direction.

For the purpose of evaluating the SSI effects on the dynamic response of the structure and identifying the natural SSI system frequency, the amplification function can be evaluated as the ratio of the horizontal response at the top of the structure and the horizontal free-field ground response, both expressed in terms of Fourier spectra. The amplification functions obtained by predicted and recorded data with reference to the NS component on motion are shown in Figure 9, together with the corresponding function as determined for the fixed-base structure analysis (without considering any SSI effects). As expected, the fixed-base natural frequency of the structure (10.66 Hz) reduces to a lower value (around 3.5 Hz) as a consequence of the compliance of the soil deposit, while the associated damping ratio increases, due to radiation and material dampings. The comparison of the predicted results to the recorded ones shows a fairly good agreement in terms of damping ratio, though the natural frequency of the SSI system is slightly over-estimated.

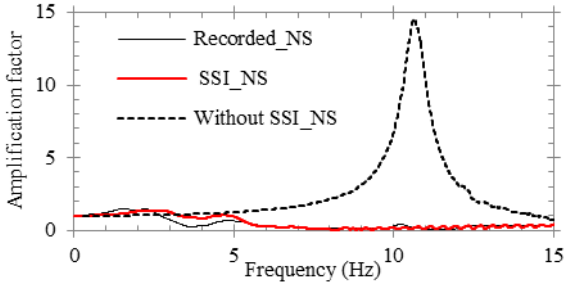

***Figure 9**. Amplification function of the structural motion to the free-field ground motion considering the effects of the SSI interaction along NS direction.*

6. Conclusions

In the present paper, a 3D FE numerical approach is proposed to back-analyse the free-field motion and the dynamic response of a small-scale structure of a nuclear power plant, recorded at Lotung (Taiwan) during the LSST7 event. The non-linear behaviour of soil is simulated by the isotropic hardening elasto-plastic model *HSsmall*, while linear visco-elasticity is assumed for the structural model. Time domain numerical analyses are performed under multidirectional conditions of the seismic motion, applying simultaneously both compo-

nents of the DHB-47 motion, recorded at the depth of 47 m from the ground surface.

Numerical results prove to be in good agreement with the free-field array's measurements at depth and at the ground surface, both in terms of peak acceleration and zero crossings. Furthermore, the main features of the dynamic structural response are also captured by the SSI numerical simulation.

The overall comparison confirms the capability of the *HSsmall* model to predict the seismic ground motion and highlights the effectiveness of the proposed numerical approach to investigate complex problems characterised by soil-structure interaction phenomena under multi-directional seismic motions.

References

[1] Veletsos A.S., Nair V.D.: Seismic interaction of structures on hysteretic foundations. *ASCE Journal of Structural Division*, Vol. 101, 1975, pp.109-129.

[2] Wolf J.P.: *Dynamic soil-structure interaction*. Englewood Cliffs, NJ: Prentice Hall; 1985.

[3] Kramer S.: *Geotechnical earthquake engineering*, Upper Saddle River, N.J.: Prentice Hall; 1996.

[4] Brinkgreve R.B.J., Engin E., Swolfs W.M.. *Plaxis 3D. Reference manual*, 2013.

[5] Brinkgreve R.B.J., Kappert M.H., Bonnier P.G.: Hysteretic damping in a small-strain stiffness model. *Proc. 10th Int. Symp. Numer. Model. Geomech. NUMOG 10*, 2007, pp. 737–742.

[6] Amorosi A., Boldini D., Falcone G.: Numerical prediction of tunnel performance during centrifuge dynamic tests. *Acta Geotechnica*, Vol. 9, 2014, pp.581–96.

[7] Amorosi A., Boldini D., di Lernia A.: Modellazione numerica della risposta sismica locale: il caso di Lotung. *XXV Convegno Naz. di Geotecnica*, Edizioni AGI; 2014, pp. 21–28.

[8] Amorosi A., Boldini D., di Lernia A.: Seismic ground response at Lotung: Hysteretic elasto-plastic-based 3D analyses. *Soil Dynamic and Earthquake Engineering*, Vol. 85, 2016, pp. 44–61.

[9] Amorosi A., Boldini D., di Lernia A.: Advanced numerical approaches to the seismic soil and structural response analyses. *Proc. SECED 2015*

"Earthquake risk Eng. Towar. a resilient world," Cambridge, UK, 2015.

[10] Tang H.T.: *Large-scale soil-structure interaction.* Report No. NP-5513-SR, Palo Alto, California, EPRI, 1987.

[11] EPRI. *Post-Earthquake analysis and data correlation for the 1/4-scale containment model of the Lotung Experiment*. Report No NP-7305-SL, Palo Alto, California, 1991

[12] EPRI. *Spatial variation of earthquake ground motion for application to Soil-Structure Interaction*. Report No TR-100463, Palo Alto, California, 1992

[13] Elgamal A.W, Zeghal M., Tang H.T., Stepp J.C.: Lotung Downhole Array. I: Evaluation of Site Dynamic Properties. *Journal of Geotechnical Engineering*, Vol. 121, 1995, pp. 350–362.

[14] Zeghal M., Elgamal A.W., Tang H.T., Stepp J.C.: Lotung Downhole Array. II: Evaluation of Soil Nonlinear Properties. *Journal of Geotechnical Engineering*, Vol. 121, 1995, pp. 363–378.

[15] Borja R.I., Chao H.Y., Montáns F.J., Lin C.H.: Nonlinear ground response at Lotung LSST site. *Journal of Geotechnical and Geoenvironmental Engineering*, Vol. 125, 1999, pp. 187–197.

[16] Borja R.I., Lin C.H., Sama K.M., Masada G.M.: Modelling non-linear ground response of non-liquefiable soils. *Earthquake Engineering and Structural Dynamics*, Vol. 29, 2000, pp. 63–83.

[17] De Mello V.F.B.: The Standard Penetration Test, State Of the Art Report. IV Panam. *Conference Soil Mechanics and Foundation Engineering*, San Juan, Puerto Rico, 1971

[18] Vucetic M., Dobry R.: Effect of Soil Plasticity on Cyclic Response. *Journal of Geotechnical Engineering, Vol. 117* 1991, pp. 89–107

[19] Schanz T., Vermeer P.A., Bonnier P.G.: The hardening soil model: formulation and verification. *Beyond 2000 in Computational Geotechnics*, 1999, pp. 281–296.

[20] Benz T.: *Small-Strain Stiffness of Soils and its numerical consequences.* PhD. Thesis, University of Stuttgart, Germany, 2006.

[21] Benz T., Vermeer P.A., Schwab R.: A small-strain overlay model. *International Journal for Numerical and Analytical Methods in Geomechanics*, Vol. 33, 2009 pp. 25–44.

[22] Hardin B.O., Drnevich V.P.: Shear Modulus and Damping in Soils. *Journal of Soil Mechanics and Foundation Division*, Vol. 98, 1972, pp. 667–92.

[23] Amorosi A., Boldini D., Elia G.: Parametric study on seismic ground response by finite element modelling. *Computers and Geotechnics*, Vol. 37, 2010, pp. 515–528.

[24] Bardet J.P., Ichii K., Lin C.H.: *EERA: A computer program for equivalent-linear earthquake site response analyses of layered soil deposits*. 2000, University of Southern California- Deparrtment of Civil Engineering.